Lasers in Medical Science (2018) 33:1673–1683
https://doi.org/10.1007/s10103-018-2513-x

ORIGINAL ARTICLE

Low-level laser irradiation induces a transcriptional myotube-like profile in C2C12 myoblasts

Juarez H. Ferreira[1] · Sarah S. Cury[1] · Ivan J. Vechetti-Júnior[1] · Geysson J. Fernandez[1] · Leonardo N. Moraes[1] · Carlos A. B. Alves[1] · Paula P. Freire[1] · Carlos E. A. Freitas[2] · Maeli Dal-Pai-Silva[1] · Robson F. Carvalho[1]

Received: 20 January 2018 / Accepted: 17 April 2018 / Published online: 2 May 2018

Abstract

Low-level laser irradiation (LLLI) has been used as a non-invasive method to improve muscular regeneration capability. However, the molecular mechanisms by which LLLI exerts these effects remain largely unknown. Here, we described global gene expression profiling analysis in C2C12 myoblasts after LLLI that identified 514 differentially expressed genes (DEG). Gene ontology and pathway analysis of the DEG revealed transcripts among categories related to cell cycle, ribosome biogenesis, response to stress, cell migration, and cell proliferation. We further intersected the DEG in C2C12 myoblasts after LLLI with publicly available transcriptomes data from myogenic differentiation studies (myoblasts vs myotube) to identify transcripts with potential effects on myogenesis. This analysis revealed 42 DEG between myoblasts and myotube that intersect with altered genes in myoblasts after LLLI. Next, we performed a hierarchical cluster analysis with this set of shared transcripts that showed that LLLI myoblasts have a myotube-like profile, clustering away from the myoblast profile. The myotube-like transcriptional profile of LLLI myoblasts was further confirmed globally considering all the transcripts detected in C2C12 myoblasts after LLLI, by bi-dimensional clustering with myotubes transcriptional profiles, and by the comparison with 154 gene sets derived from previous published in vitro omics data. In conclusion, we demonstrate for the first time that LLLI regulates a set of mRNAs that control myoblast proliferation and differentiation into myotubes. Importantly, this set of mRNAs revealed a myotube-like transcriptional profile in LLLI myoblasts and provide new insights to the understanding of the molecular mechanisms underlying the effects of LLLI on skeletal muscle cells.

Keywords Transcriptome · Laser treatment · Muscle regeneration · Myogenesis · RNA sequencing

Introduction

Low-level light therapy consists of the application of a low-power light source (laser or LED) to different purposes such as stimulate tissue repair, decrease inflammation and edema, and as an analgesic [1]. The cellular and molecular mechanisms of action are largely unknown, but chromophores such as cytochrome c oxidase and light-sensitive ion channels have been implicated in the activation of signaling pathways after light exposure [2–4]. Considering these light effects on biological systems, low-level laser irradiation (LLLI) has been used as a non-invasive method to promote or accelerate skeletal muscle regeneration capability [5–9]. Skeletal muscle regeneration is mainly accomplished by the proliferation and differentiation of myogenic cells derived from satellite cells (reviewed in [10]). After trauma or injury, satellite cells are activated, and become immature muscle cells or myoblasts that proliferate, migrate, and fuse into existing muscle fibers, or form new myofibers during muscle repair [11]. Consequently, several studies have been conducted in satellite cells and myogenic cell lines to understand the biological effects of LLLI on cellular and molecular mechanisms that contribute to muscle regeneration [12–16]. These studies clearly demonstrate that myogenic cells modulate proliferation and differentiation, and change the expression of myogenic regulatory factors and cell cycle

Electronic supplementary material The online version of this article (https://doi.org/10.1007/s10103-018-2513-x) contains supplementary material, which is available to authorized users.

✉ Robson F. Carvalho
rcarvalho@ibb.unesp.br

[1] Department of Morphology, Institute of Biosciences, São Paulo State University (UNESP), Botucatu, SP, Brazil

[2] Department of Physiotherapy, University of Western Sao Paulo (UNOESTE), Presidente Prudente, SP, Brazil

regulatory proteins in response to LLLI. Although the increasing evidence of the beneficial effects of LLLI on myogenic cells has become widely accepted, the global regulatory molecular mechanisms by which LLLI exerts these effects remain largely unknown.

Previous examinations of large scale mRNA expression generated by cDNA microarray analysis have generated insights on the molecular changes underlying the effects of LLLI in different cells types. For example, the expression levels of various genes involved in cell proliferation, apoptosis, and the cell cycle were affected by LLLI in mesenchymal stem cells [17]. Similarly, several differentially expressed genes (DEG) were identified in human fibroblasts after low-intensity red light; most of these genes either directly or indirectly participate in biologic processes related to cellular proliferation [18]. However, to the best of our knowledge, no other study has used a global mRNA expression profiling analysis by high-throughput RNA sequencing (RNA-Seq) method to study the effects of LLLI in skeletal muscle cells. This approach may provide meaningful insights into how LLLI exerts its regulatory effects in these cells and unravels laser-stimulated networks and molecular pathways. Therefore, our goal was to perform a global mRNA expression profiling analysis in C2C12 myoblasts after LLLI.

Materials and methods

Cell culture

C2C12 myoblasts were maintained in growth medium Dulbecco's modified Eagle medium (DMEM) supplemented with 10% fetal bovine serum (Thermo Scientific, USA), 100 IU/mL penicillin, and 100 μg/mL streptomycin in a humidified incubator at 37 °C with 5% CO_2. After reaching 70–80% confluence, cells were washed in phosphate-buffered saline (PBS), trypsinized, centrifuged (1500 rpm, 10 min, 4 °C), resuspended in DMEM medium with FBS 10%, and counted in Neubauer chamber. Subsequently, the cells were transferred and cultured into 6-well plates (1×10^5 cells/well) or 96-well plates (and 5×10^3 cells/well) in 96-well plates, according to the experiments.

Laser irradiation

Cells were divided into two experimental groups: non-irradiated control group (CT, $n = 3$) and low-level laser irradiated group (LLL, $n = 3$). The LLL cells were submitted to a gallium-aluminum-arsenide (GaAlAs) diode laser, with 660-nm wavelength, output power of 20 mW, beam area of 0.035 cm^2, and an energy density of 2 J/cm^2. The time of exposure was 3 s/point. Each well plate was irradiated in 33 points (6-well plate) or 1 point (96-well plate) to ensure the complete irradiation over the entire cell-culture plate. The CT group was subjected to the same experimental conditions as the LLL, except for the irradiation. Irradiation was performed in the dark to avoid the influence of other light sources, and the beam incidence angle was positioned perpendicularly (90°) at 1 cm of lower surface plate to the irradiation.

Cell viability assay

The viability of the proliferating C2C12 myoblasts, after LLLI, was assessed by using the 3-(4,5-dimethylthiazol-2-yl)-2,5-diphenyltetrazolium bromide (MTT) assay (Sigma-Aldrich, USA). This assay measures the activity of living cells via mitochondrial dehydrogenase activity that reduces MTT to purple formazan. The cells were seeded in a 96-well plate with DMEN, and at 0, 6, 12, 24, and 48 h after LLLI, MTT (0.5 mg/mL) in phosphate-buffered saline was added to each well. Following, 100 μL of DMSO was added to each well to dissolve formazan crystals. The solution absorbance was measured at 570 nm using a microplate reader (2020, Anthos Labtec Instruments, Austria).

Scratch assay

C2C12 myoblasts were plated in 6-well plate and cultured in DMEM until reaching 80–90% confluence. Subsequently, a single-line scratch was mechanically generated in a cell monolayer by a 200-μl plastic tip. Cell debris were removed through two PBS washes, and 2 mL of DMEM supplemented with 5% fetal bovine serum was added to each well, when the LLL group was irradiated. The scratch open area was photographed and analyzed at 0, 6, 12, 24, and 48 h after LLLI, and the scratch closure rate was determined by plotting the open scratch area changes as a function of the time.

5-Bromo-2′-deoxyuridine incorporation

C2C12 myoblasts were plated on a glass coverslip until reaching 70–80% confluence in DMEM and then were irradiated and incubated at 37 °C with 5% CO_2 for 5 h; subsequently, the medium was changed to a DMEM containing 10 μM 5-Bromo-2′-deoxyuridine (BrdU) (Sigma-Aldrich, USA) for 60 min. Cells were then fixed in 4% paraformaldehyde, permeabilized with 0.1% Triton X-100 in PBS and blocked for 1 h in 10% goat serum, 1% Triton X-100 in PBS, denatured with 2 N HCl in PBS containing 0.5% Triton X-100 at 37 °C, for 30 min, and neutralized with 0.1 M borate buffer pH 8,5 for 10 min. Subsequently, the cells were incubated with mouse anti-BrdU antibody (diluted 1:1000; Sigma-Aldrich, USA), for 1 h, and next, the cells were incubated overnight in incubation solution (5% goat serum, 0.3% Triton X-100) at 4 °C. Finally, goat anti-mouse IgG Texas red-conjugated (1:5000; Santa Cruz Biotechnology USA)

were added to the cells for 1 h at room temperature, and coverslips were mounted using Vectashield (Vector Labs, USA). Cells were counted in a fluorescent inverted microscope (BX61 Olympus, Japan) to calculate the ratio of $BrdU^+$ cells to the total cell number.

Total RNA extraction

Total RNA extraction was performed using TRIZOL kit (Thermo Fisher, USA) according to the manufacturer's instructions. The RNA was quantitated by spectrophotometry using NanoVue (GE Healthcare Life Sciences, USA) and the quality of RNA was obtained by the RNA integrity number (RIN) from the analysis of ribosomal RNAs based on microfluidics, using the 2100 Bioanalyzer system (Agilent, USA).

RNA sequencing

Total RNA (5 μg) were used to construct RNA-Seq libraries for CT ($n = 3$) and LLL ($n = 3$) groups that were sequenced in a same flow cell, as paired-end, 2 × 100 bp, on an Illumina HiScanSQ instrument (Illumina, USA), following manufacturer's instructions, which generated an average of 25 million paired-end reads per sample. The raw sequence files (.fastq files) underwent quality control analysis using FastQC and average Phred quality scores of ≥ 20 per position were used for alignment. The raw paired-end reads of the cDNA fragments were aligned to the mouse transcriptome (RefSeq, mm10) using the TopHat (version 1.3.2) spliced junction discovery tool [19]. The Python package HTSeq was used to count mapped reads to each transcript, and the differential expression across CT and LLL groups were identified using DEseq (version 1.22.1) and reported as fold change along with associated *p*-values. Cut-offs for significant changes were a fold change > 1.2 and a p value ≤ 0.05. The analyses were performed with software package R (http://www.r-project.org).

Pathway and gene ontology enrichment analysis

To further understand the biological relevance of differential expressed genes, we performed functional enrichment analysis in the context of the Gene Ontology (GO) categories, Kyoto Encyclopedia of Genes and Genomes (KEGG), Reactome, and WikiPathways databases. Pathway analysis was performed using Cytoscape (v.3.4.0) [20] with ClueGO (version 2.2.5) packages [21]. A p value cut-off of 0.05 by group and fold enrichment greater than 10% were used to identify the enriched categories. A kappa score was calculated to reflect the relationships between the terms based on the similarity of their associated genes, and PSIQUIC web services with the threshold set at 0.3 was used to provide a comprehensive view on the relevant pathways using experimental and in silico data from gene networks, protein–protein interactions, and functional interactions [22, 23].

Identification of transcriptionally similar muscle gene sets

Transcriptionally similar gene sets to the differentially expressed genes in C2C12 myoblasts after LLLI were identified by the comparison with 154 gene sets derived from published in vitro muscle microarray studies, available at SysMyo Muscle Gene Sets (http://www.sys-myo.com/). The analysis of the SysMyo Muscle Gene Sets was carried out by using Enrichr, a comprehensive gene set enrichment analysis web tools (http://amp.pharm.mssm.edu/Enrichr/) [24, 25].

Statistical analysis

All data are presented as mean ± SD. Differences between treated and nontreated cells were analyzed using multiple t tests with Sidak-Bonferroni correction. $p < 0.05$ was considered statistically significant. The calculations and artwork were made using GraphPad software (version 6.01). Venn diagrams were created and analyzed with Venny web Server 2.1 (http://bioinfogp.cnb.csic.es/tools/venny/index.html).

Results

Low-level laser irradiation does not affect cell viability but reduces migration and proliferation of C2C12 myoblasts

We found no significant effects on C2C12 myoblasts viability by MTT assay at 0, 6, 12, 24, and 48 h after LLLI (Fig. 1a). C2C12 myoblast migration and proliferation were indirectly evaluated by scratch assay at 0, 6, 12, 24, and 48 h after LLLI treatment (Fig. 1b). C2C12 myoblasts exposed to LLLI showed significantly decreased scratch closure rate at 6, 12, and 24 h, when compared to the control group ($p < 0.05$) (Fig. 1c). Considering these results, we selected the time point 6 h after LLLI for the further analyses. Next, C2C12 myoblast proliferation was measured by BrdU incorporation (Fig. 1d), which showed a decreased C2C12 myoblast proliferation ratio at 6 h after LLLI ($p < 0.05$) (Fig. 1e).

LLLI promotes transcriptional changes in C2C12 myoblasts

To understand the transcriptome changes associated with LLLI on C2C12 myoblasts, we performed a global mRNA expression profiling that detected a total of 39,179 transcripts. Differential expressed genes between

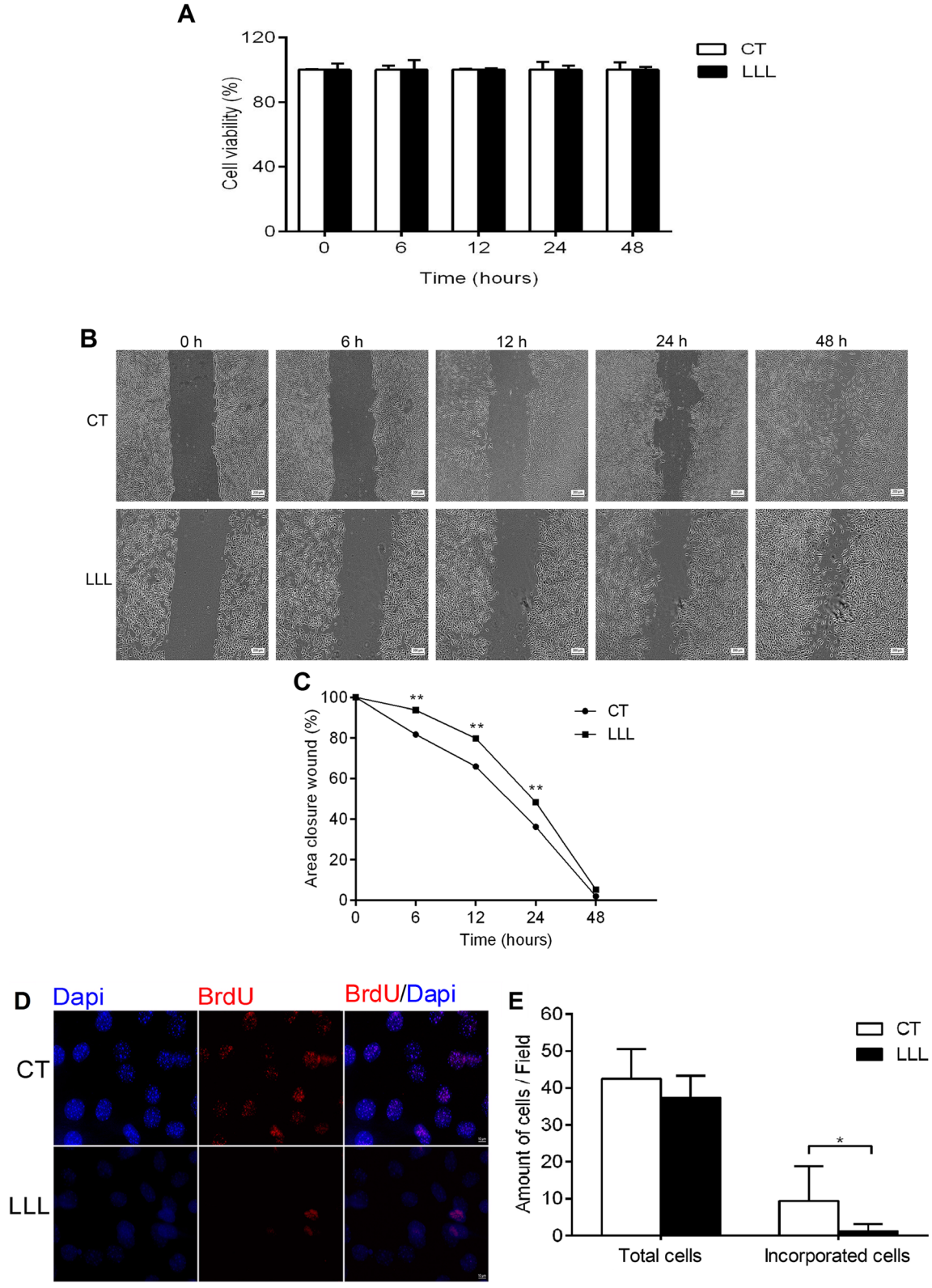

LLL and CT groups were selected and ranked by a combination of fold change ≥ 1.2 and adjusted p value < 0.05 cut-off (Online Resource 1). LLLI affected the expression of 514 genes, out of which 263 and 251 were up- and down-regulated, respectively (Online Resource 1). Remarkably, the unsupervised hierarchical clustering analysis of the mRNA expression data demonstrated biological triplicate clustering and a clear segregation

◀ **Fig. 1** Low-level laser irradiation (LLLI) does not affect cell viability but reduces migration and proliferation of C2C12 myoblasts. **a** Cellular viability rate analyzed by MTT assay after the LLLI of C2C12 myoblasts. Cellular viability rate was quantified considering the absorbance variation per hour between 6, 12, 24, and 48 h related to the initial absorbance (time 0 h). **b** Cellular migration and proliferation were indirectly measured by a scratch assay after LLLI of C2C12 myoblasts at 0, 6, 12, 24, and 48 h post-scratch. **c** The scratch closure was quantified by measuring the remaining unmigrated area and is expressed as relative percentage (%). **d** Cellular proliferation was analyzed by BrdU incorporation (red) detected 6 h after LLLI on the C2C12 myoblasts. Nuclei are counter-stained with DAPI (blue). **e** Number of BrdU+ cells per group after LLLI. Data represent mean of three independent experiments, and bars represent the standard deviation. Statistical significance was analyzed by Student's *t* tests. $*p < 0.05$, $**p < 0.002$

between CT and LLL groups (Fig. 2). All samples used in the RNA sequencing experiment presented a RIN ≥ 9.5.

LLLI induces changes in the expression of genes associated with different functional categories

To determine the biological and functional implications of the expression changes induced by LLLI treatment in C2C12 myoblasts, we performed a functional enrichment analysis on the set of DEG (Online Resource 2). This enrichment functional analysis in C2C12 myoblasts exposed to LLLI revealed categories related to cell cycle, cell migration, response to stress, muscle cell proliferation, ribosome biogenesis, anatomical structure, DNA metabolic process, cell death, and blood vessel development (Fig. 3).

To further understand the individual pathways, we also investigated the over- and under-expressed genes in each pathway. Interestingly, this analysis revealed that cell cycle pathway presented the higher enrichment (60%), and all the genes classified in this category were down-regulated (Fig. 3).

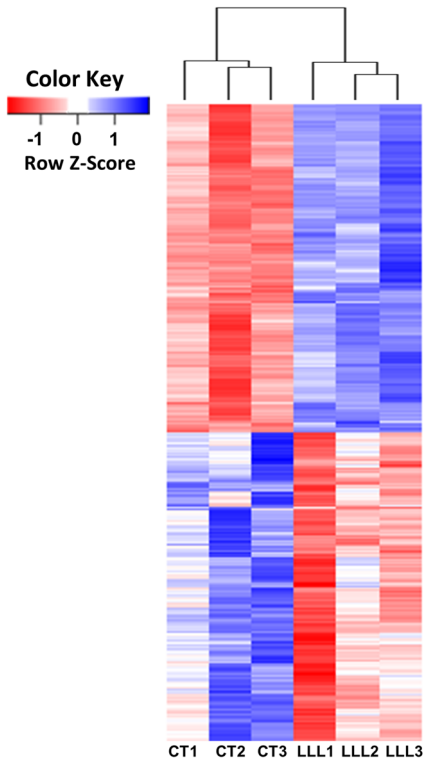

Fig. 2 Low-level laser irradiation (LLLI) promotes transcriptional changes in C2C12 myoblasts. Heatmap of mRNA expression levels for the differentially expressed genes (DEG) between LLL and CT groups (1, 2, and 3 represent independent biological replicates for each group). Unsupervised hierarchical clustering analysis was performed using DEG with p value < 0.05 and fold change > 1.2 and are shown as a color scale

LLLI induces distinct cell type-specific transcriptional changes

Next, we evaluated whether the gene expression changes induced by LLLI treatment in C2C12 myoblasts are distinct from different cell types that were also irradiate with LLLI. For this purpose, we compared our RNA-Seq data with previous microarray studies that have evaluated the effect of (1) LLLI on mesenchymal stem cell (MSCs) [17] and (2) red light irradiation on human fibroblasts (HS27) [18]. The intersection of the three studies tested showed no overlapping transcripts (Fig. 4a); however, LLLI-treated myoblast had six DEG (Ada, Ccnd1, Cfh, Creld1, Gfer, and Wdr12) in common with MSCs [17], and three (Ahcy, Ppih, and Serpine1) with the HS27 [18] (Fig. 4a). We also performed functional enrichment analysis on the DEG in HS27 and MSCs cells to determine the functional categories and pathways associated with LLLI treatment in these cells and, finally, we compared these results with our data. This analysis showed no overlapping functional categories and pathways, indicating that that LLLI induces distinct functional categories that are cell type-specific (Online Resource 3). Moreover, comparing our RNA-Seq data with the transcriptome data generated by microarrays technique in HS27 and MSCs [17, 18], our data presented a higher number of DEG in C2C12 (Fig. 4a) and, consequently, we were able to identify a higher number of functional categories after LLLI (Fig. 4b).

LLLI induces a transcriptional myotube-like profile in C2C12 myoblasts

Considering the number of previous studies that have indicated the potential effects of LLLI on myogenesis, we compared our RNA-Seq data with literature data and asked whether a sub-set of genes in LLLI-treated myoblasts overlaps with data from two myogenesis studies

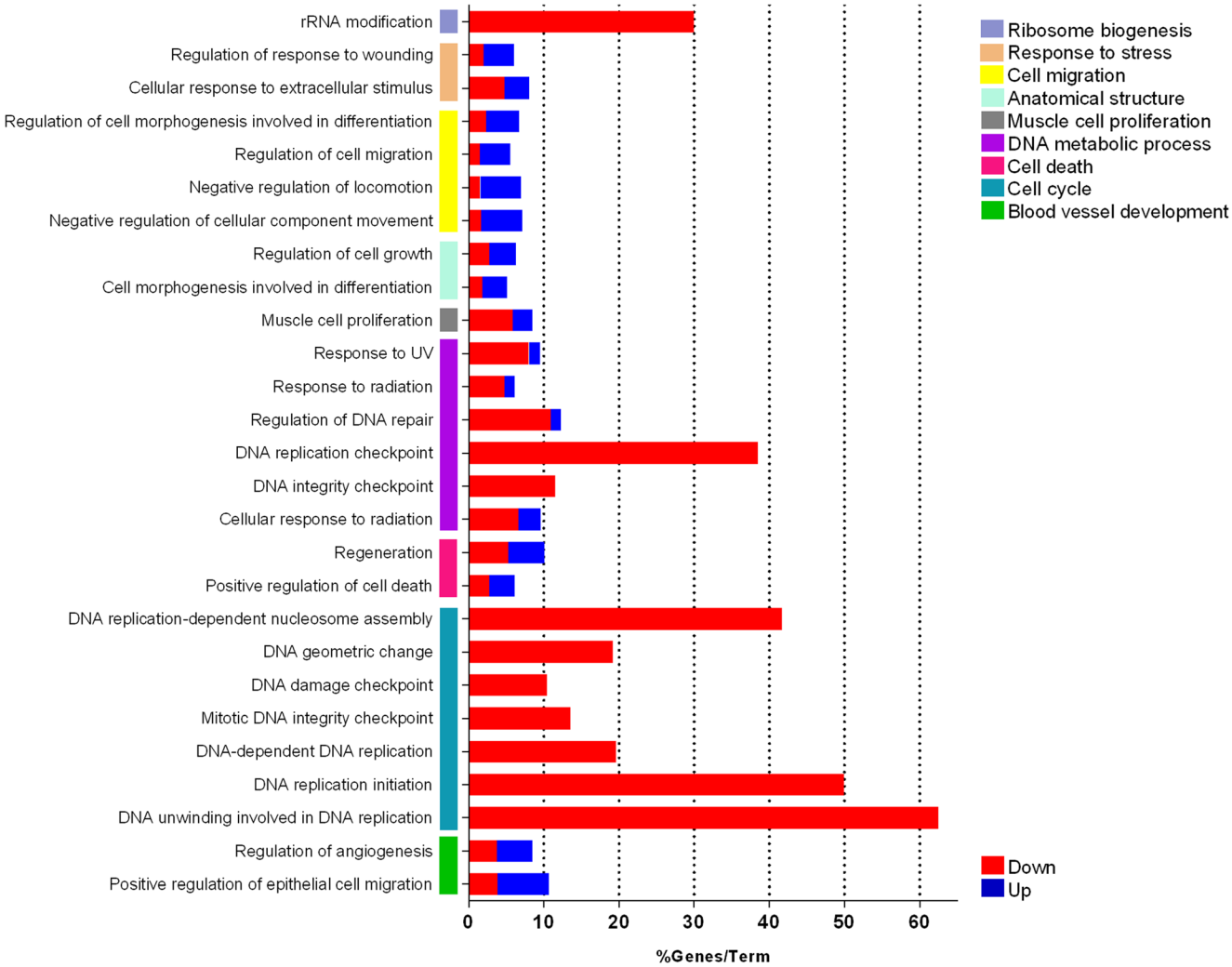

Fig. 3 Low-level laser irradiation (LLLI) induces changes in the expression of genes associated with different functional categories. Pathway and gene ontology enrichment analysis of the differentially expressed genes (DEG) in C2C12 myoblasts after LLLI to identify top pathways and ontologies. Each vertical colored bar (*y*-axis) represents a major module; horizontal bars represent the percentage of genes presented in the data set compared to the total number of genes in each pathway/ontology. Fractions of the DEG in each pathway (red/down, blue/up; respectively) are shown in *x*-axis

[26, 27] with datasets stored at Gene Expression Omnibus (GEO; https://www.ncbi.nlm.nih.gov/gds). These studies used global microarray analysis to evaluate the transcriptome changes during myogenesis (myoblasts and myotubes), and the data are accessible at NCBI GEO database [26, 27] by the following accession numbers: GSE3243 (not published) and GEO990 [28]. Initially, using the dataset from these two myogenesis studies, we selected the set of DEG between myoblasts and myotubes to intersect with the genes that were changed in myoblasts after LLLI. This intersection showed a total of 42 transcripts in our data that overlaps with DEG in myotubes from GSE3243 and GEO990 (Fig. 5a). Moreover, a total of 151 transcripts in our LLLI-treated myoblasts data overlaps with the DEG in myotubes from the GSE990 [28] dataset, and with 89 transcripts with the DEG in myotubes from the GSE3243 dataset (Fig. 5a). We also compared these DEG that specifically overlap with the corresponding protein products from a study that evaluated the effect of LLLI on global protein expression in C2C12 myoblasts [14]. However, the proteomic data resulted in a lower number of overlapping to predict a transcriptional *myotube-like* profile. The intersection of all the four conditions tested revealed that only the protein proliferation-associated protein 2G4 (Pa2g4), present in the proteomic study, overlaps with its corresponding transcript in the conditions that were tested (Fig. 5a).

Next, we performed a hierarchical cluster analysis with the 42 transcripts differentially expressed that overlap between GSE3243, GSE990 [28], and our data by using Euclidean distance similarity. This clustering analysis showed that the LLLI-treated myoblasts have a myotube-like profile, clustering away from the myoblast profile (Fig. 5b). Importantly, the

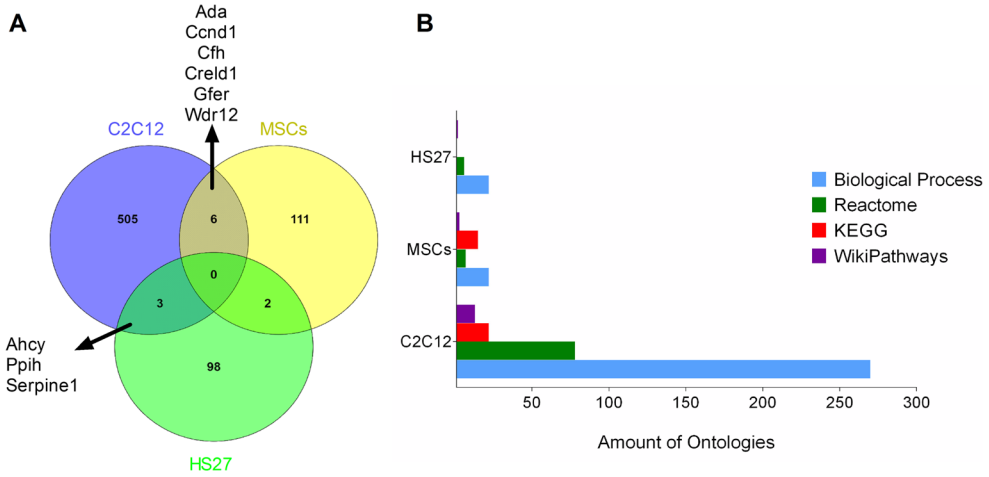

Fig. 4 Low-level laser irradiation (LLLI) induces cell type-specific transcriptional changes of distinct functional categories. Comparison of our RNA-Seq data (C2C12 myoblasts after LLLI) with previous microarray studies that have evaluated the effect of (1) LLLI on mesenchymal stem cell (MSCs) [17] and (2) red light irradiation on human fibroblasts (HS27) [18]. **a** Veen diagram showing the overlap of genes change in C2C12 myoblasts, HS27, and MSC. **b** Functional enrichment analysis on the differentially expressed genes in HS27 and MSC cells was used to determine the functional categories and pathways associated with LLLI treatment in these cells, which were compared with our data (C2C12 cells). Each horizontal bar represents the quantity of enriched ontology terms presented in the data set

myotube-like transcriptional profile of the LLLI myoblasts was globally confirmed by a bi-dimensional clustering of the 1156 transcripts detected in our RNA-Seq data that specifically overlaps with the DEG from the GSE990 [28] dataset (Fig. 5c). To further confirm the global myotube-like transcriptional profile of the LLLI myoblasts, we also compared the differentially expressed genes in C2C12 myoblasts after LLLI with 154 gene sets derived from published in vitro muscle microarray studies. This analysis revealed that, out of the 25 top-ranked most transcriptionally similar gene sets (overlapping genes) to the 514 DEG in myoblasts after LLLI, 23 are derived from differentiated myotubes and one is from a cardiotoxin injury model for the study of muscle regeneration in mice [29] (Online Resource 4).

Discussion

Several studies have indicated that LLLI affects skeletal muscle cell proliferation and differentiation in vivo and in vitro. Although the therapeutic value of LLLI has become widely accepted, the global regulatory molecular mechanisms by which it exerts these effects on skeletal muscle cells remain largely unknown. In a comprehensive examination of global mRNA expression levels, we identified a large set of mRNAs that respond to changes following C2C12 myoblast LLLI and appear to play an important role in myoblast proliferation and differentiation into myotubes. Furthermore, we demonstrated that the LLLI effects on C2C12 myoblast differentially regulate mRNAs that reveal a myotube-like transcriptional profile, generating further insights on the specific molecular changes underlying the effects of LLLI on skeletal muscle cells.

Initially, based on migration, proliferation, and cell viability parameters, we selected an appropriate time point, at 6 h post a single exposure of C2C12 cells to the laser radiation, to proceed to the transcriptomic analysis. These analyses showed that, after 6 h of LLLI, C2C12 myoblasts presented reduced migration and proliferation without affecting cell viability. These results are in accordance with a previous study performed in C2C12 cells, which also showed that laser treatment induced a decrease in the cell proliferation rate without affecting cell viability, while leading to the expression of the early differentiation marker MyoD [14]. LLLI also has the potential to increase the survival of primary myogenic donor cells, promote their fusion with the host myofibers, and enhance their ability to recover [15]. Interestingly, LLLI in association with *Bothrops jararacussu* venom has been shown to promote C2C12 differentiation by up-regulating myogenic factors [30].

On the other hand, Ben-Dov et al. [16] demonstrated that LLLI on primary rat satellite cell cultures induced cell cycle regulatory protein expression, increased satellite cell proliferation, and inhibited cell differentiation. LLLI also stimulated cell cycle entry and the accumulation of satellite cells around isolated single fibers [13]. Variable effects were achieved in a same study that used different LED light wavelengths, with blue (470 nm) or red (630 nm) LED light illumination decreasing or increasing C2C12 proliferation rates, respectively [12]. While there are no simple explanations to the apparent inconsistencies among these studies that have evaluated the effect of LLLI on proliferation and differentiation of skeletal muscle myogenic cells, it is clear that LLLI affects these processes and promotes or accelerates skeletal muscle regeneration [5–9].

To the best of our knowledge, this is the first global transcriptome catalogue of skeletal muscle cells after LLLI. Our

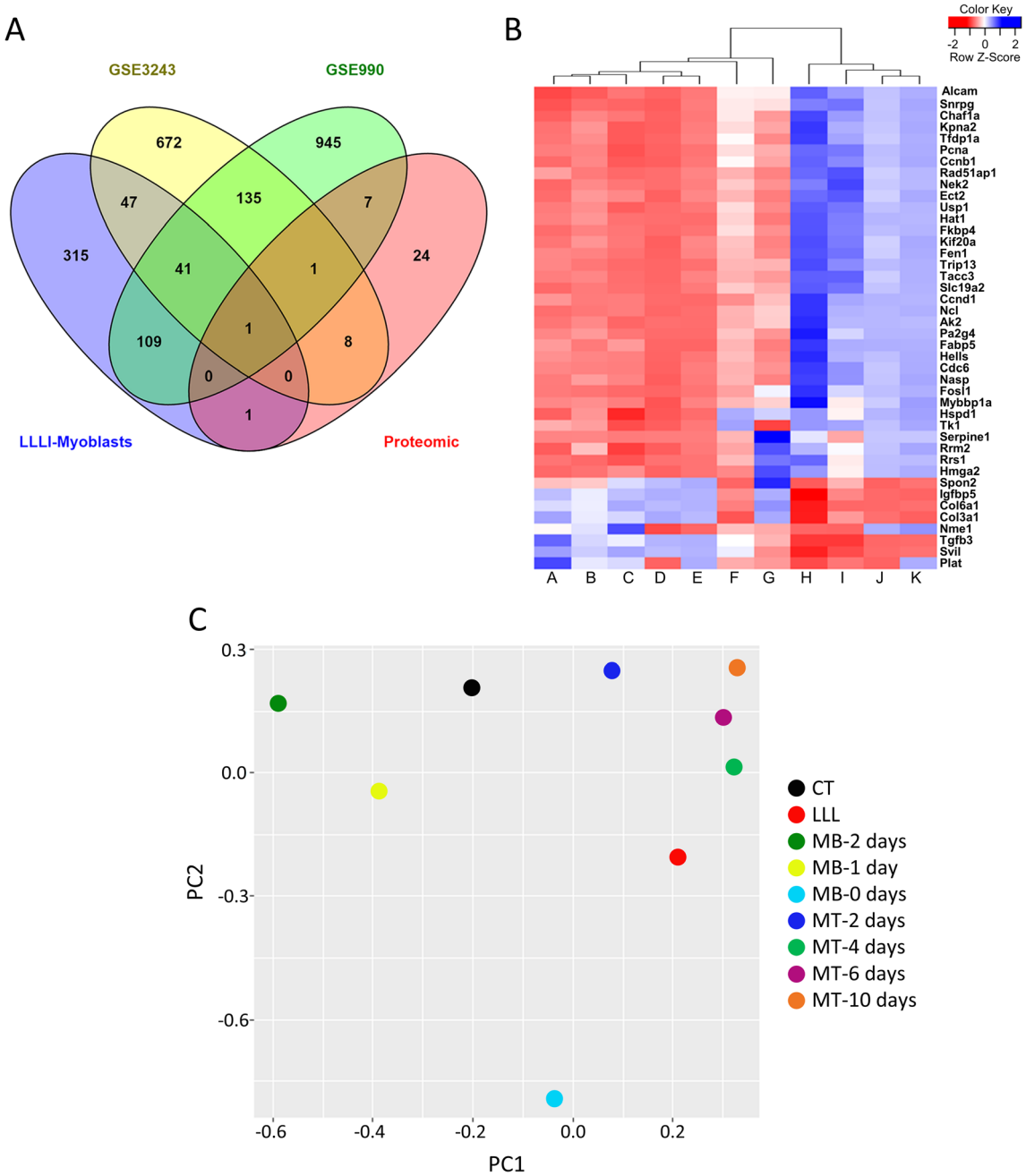

Fig. 5 Low-level laser irradiation (LLLI) LLLI induces a transcriptional myotube-like profile in C2C12 myoblasts. **a** Venn diagram showing the differentially expressed genes (DEG) of our RNA-Seq data from LLLI-treated myoblasts that overlaps with global microarrays data from two previously published studies that have evaluated the transcriptome changes during myogenesis (DEG between myoblasts and myotubes). These data are accessible at NCBI GEO database by the following accession numbers: GSE3243 (not published) and GEO990 [28]. The DEG from the three transcriptomics studies are also compared with the corresponding protein products from a study that evaluated the effect of LLLI on global protein expression in C2C12 myoblasts [14]. **b** Clustering analysis of the 42 DEG of our RNA-Seq data from LLLI-treated myoblasts that are shared with GSE3243 and GEO990 [22]. GSE990 myotubes: A = 10 days, B = 6 days, C = 4 days, and F = 2 days; GSE990 myoblasts: G = 0 days, H = − 2 days, and I = − 1 day; GSE3243 myotube: D = 4 days; and GSE3243 myoblast: K = − 2 days; LLLI myoblast: E = LLL group; and myoblasts: J = control group. **c** Principal component analysis (PCA) for clustering the global gene expression data from LLLI myoblasts with the transcriptomic data from the in vitro myogenesis study (myoblasts and myotubes) conducted by Tomczak et al. [22] (GSE990). CT control group, LLL low-level laser group, MB myoblast, MT myotube

RNA-Seq analysis identified 514 DEG (p value < 0.05 and fold change ≥ 1.2), of which 263 and 251 were up- or down-regulated, respectively. Importantly, the unsupervised hierarchical clustering analysis of the mRNA expression data in C2C12 LLLI-treated myoblasts showed a biological replicate clustering and a segregation between CT and LLL groups.

These data clearly indicate that the LLLI effects on myoblasts transcriptional regulation are not random, and that RNA-Seq is a powerful tool to evaluate transcriptional changes promoted by LLLI in cultured cells.

Previously, Wu et al. [17] used a microarray analysis to identify transcriptome changes induced by LLLI in cultured mesenchymal stem cells, and identified 119 DEG (fold change ≥ 1.2). Zhang et al. [18] also used microarray analysis to study the effect of LLLI on cultured human fibroblasts, and found 111 DEG by more than twofold. Noteworthy, the transcriptome changes between non-irradiated and irradiated in these previous studies show very few DEG in common. Our data from LLLI-treated myoblast had six DEG in common with one study [17], and three with the other [18]. Moreover, our RNA-Seq data identified a higher number of DEG when compared to these two previous microarray studies. Accordingly, our functional analysis also presented a higher number of categories that includes cell cycle, cell migration, response to stress, muscle cell proliferation, ribosome biogenesis, anatomical structure, DNA metabolic process, cell death, and blood vessel development. The comparison of these functional categories in which the DEG are classified may help to identify shared core molecular mechanisms underlying the effects of LLLI in different cell types. However, we did not identify functional categories affected by LLLI that overlap with C2C12 myoblasts when compared with mesenchymal stem cells [17] and fibroblasts [18]. These disparities in the number of the DEG and functional pathways among the studies may occur due to the different cells types or statistical cut-offs, or several laser-related factors such as wavelength of radiation, energy density, and time of irradiation.

To further validate our RNA-Seq results and better understand the effects of LLLI on myoblasts, we asked whether a sub-set of DEG in LLLI myoblasts overlaps with Geo Expression Omnibus dataset (GEO990 [28] and GSE3243) experiments that evaluated transcriptome changes during in vitro myogenesis (myoblasts vs myotubes). Our LLLI myoblasts data had 151 transcripts in common with one dataset (GEO990), 89 transcripts with the other (GSE3243), and 42 transcripts that overlap with both datasets. Although included in different functional categories, these 42 transcripts are useful to indicate alterations triggered by LLLI in myoblast. It is interesting to note that, besides no changes in the expression of the myogenic regulatory factors (MRFs) that control myogenesis and regeneration [31], we found Hmga2 and Ccnd1 among the deregulated genes after LLLI; both were down-regulated and associated with ontology groups such as cellular response to irradiation, DNA damage checkpoint, regeneration, and cell morphogenesis involved in differentiation. Importantly, several studies have demonstrated a key role for Ccnd1 in promoting myoblast cell cycle withdrawal and terminal differentiation into myotubes [32–37]. Hmga2 has been also directly the regulation of connected to myoblast proliferation and differentiation; Hmga2 increase is coincident with satellite cell activation, and later its expression significantly declines correlating with fusion of myoblasts into myotubes [38]. Also, in accordance with these literature data, our ontology analysis revealed that cell cycle pathway presented the higher enrichment (60%), and all the genes classified in this category were down-regulated. Together, these findings indicate that LLLI in C2C12 myoblast LLLI appear to play an important role in reducing myoblast proliferation and inducing differentiation into myotubes.

Next, we performed a hierarchical cluster analysis with those 42 transcripts differentially expressed that overlap between GSE3243, GSE990 [28], and our data by using Euclidean distance similarity. Noteworthy, this clustering analysis confirmed that the LLLI myoblasts have a transcriptional *myotube-like profile*, clustering away from the myoblast profile. Monici et al. (2013) [14] previously showed that laser treatment decreased cell proliferation associated with changes of cell morphology and cytoskeletal architecture leading to the formation of tube-like structures. These authors also evaluated the effect of LLLI on global protein expression in C2C12 myoblasts and identified 42 differently expressed proteins in LLLI myoblasts. However, when we analyzed the DEG (GSE3243, GSE990 [28], and our data) that overlap with the corresponding protein products from Monici et al. (2013) [14], the proteomic data resulted in a lower number of overlapping to predict a transcriptional *myotube-like profile*. The intersection of all the four conditions tested also revealed that only the protein proliferation-associated protein 2G4 (Pa2g4) overlaps in all conditions. Pa2g4, also known as Ebp1, is expressed during myogenesis in satellite cells; however, its knockdown inhibits both proliferation and differentiation of C2C12 myoblasts and satellite cells, which also present a reduced capacity of myotube formation [39].

We also compared the differentially expressed genes in C2C12 myoblasts after LLLI with 154 gene sets derived from published in vitro muscle microarray studies available at Gene Expression Omnibus to confirm a global *myotube-like transcriptional profile* of the LLLI myoblasts. These analyses further demonstrated that all 514 DEG in myoblasts after LLLI highly overlap with gene sets of differentiated myotubes from the study of Tomczak et al. [40], but surprisingly, also overlaps specifically with additional 22 gene sets from differentiated myotubes, and with one cardiotoxin injury model used to study muscle regeneration in mice [29].

Although our study design has proven useful, there were also limitations that must be considered. Specifically, there is a diversity of studies that analyze the effects of LLLI on C2C12 myoblasts and other cell types. These studies apply several different laser-related parameters such as wavelength of radiation, energy density, and time of irradiation, making it difficult to select specific parameters to become the results comparable. Thus, further studies are needed to better establish

how these laser-related parameters globally affect cellular and molecular mechanism in different cell types.

In summary, we demonstrate for the first time that LLLI regulates a set of mRNAs that control myoblast proliferation and differentiation into myotubes. Importantly, this set of mRNAs revealed a myotube-like transcriptional profile in LLLI myoblasts and provide new insights to the understanding of the molecular mechanisms underlying the effects of LLLI on skeletal muscle cells.

Funding This study was supported by grants from the São Paulo Research Foundation Brazil (FAPESP no. 2012/13961-6) and National Council for Scientific and Technological Development (CNPq no. 476399/2013-0).

Compliance with ethical standards

Conflict of interest The authors declare that they have no conflict of interest.

Ethical approval This article does not contain any studies with animals performed by any of the authors.

References

1. Chung H, Dai T, Sharma SK et al (2012) The nuts and bolts of low-level laser (light) therapy. Ann Biomed Eng 40:516–533. https://doi.org/10.1007/s10439-011-0454-7
2. Wang X, Tian F, Soni SS et al (2016) Interplay between up-regulation of cytochrome-c-oxidase and hemoglobin oxygenation induced by near-infrared laser. Sci Rep 6:1–10. https://doi.org/10.1038/srep30540
3. de Freitas LF, Hamblin MR (2016) Proposed mechanisms of photobiomodulation or low-level light therapy. IEEE J Sel Top Quantum Electron 22:348–364. https://doi.org/10.1109/JSTQE.2016.2561201
4. Wang Y, Huang YY, Wang Y et al (2017) Photobiomodulation of human adipose-derived stem cells using 810 nm and 980 nm lasers operates via different mechanisms of action. Biochim Biophys Acta, Gen Subj 1861:441–449. https://doi.org/10.1016/j.bbagen.2016.10.008
5. Vatansever F, Rodrigues NC, Assis LL et al (2012) Low intensity laser therapy accelerates muscle regeneration in aged rats. Photonics Lasers Med 1:287–297. https://doi.org/10.1515/plm-2012-0035
6. Assis L, Moretti AIS, Abrahão TB et al (2013) Low-level laser therapy (808 nm) contributes to muscle regeneration and prevents fibrosis in rat tibialis anterior muscle after cryolesion. Lasers Med Sci 28:947–955. https://doi.org/10.1007/s10103-012-1183-3
7. de Freitas CEA, Bertaglia RS, Vechetti Júnior IJ et al (2015) High final energy of low-level gallium arsenide laser therapy enhances skeletal muscle recovery without a positive effect on collagen remodeling. Photochem Photobiol 91:n/a-n/a. https://doi.org/10.1111/php.12446
8. Amaral AC, Parizotto NA, Salvini TF (2001) Dose-dependency of low-energy HeNe laser effect in regeneration of skeletal muscle in mice. Lasers Med Sci 16:44–51
9. Weiss N, Oron U (1992) Enhancement of muscle regeneration in the rat gastrocnemius muscle by low energy laser irradiation. Anat Embryol (Berl) 186:497–503
10. Buckingham M (2006) Myogenic progenitor cells and skeletal myogenesis in vertebrates. Curr Opin Genet Dev 16:525–532. https://doi.org/10.1016/j.gde.2006.08.008
11. Wang YX, Rudnicki MA (2011) Satellite cells, the engines of muscle repair. Nat Rev Mol Cell Biol 13:127–133. https://doi.org/10.1038/nrm3265
12. Teuschl A, Balmayor ER, Redl H et al (2015) Phototherapy with LED light modulates healing processes in an in vitro scratch-wound model using 3 different cell types. Dermatologic Surg 41:261–268. https://doi.org/10.1097/DSS.0000000000000266
13. Shefer G, Partridge TA, Heslop L et al (2002) Low-energy laser irradiation promotes the survival and cell cycle entry of skeletal muscle satellite cells. J Cell Sci 115:1461–1469
14. Monici M, Cialdai F, Ranaldi F et al (2013) Effect of IR laser on myoblasts: a proteomic study. Mol BioSyst 9:1147–1161. https://doi.org/10.1039/c2mb25398d
15. Shefer G, Ben-Dov N, Halevy O, Oron U (2008) Primary myogenic cells see the light: improved survival of transplanted myogenic cells following low energy laser irradiation. Lasers Surg Med 40:38–45. https://doi.org/10.1002/lsm.20588
16. Ben-Dov N, Shefer G, Irinitchev A et al (1999) Low-energy laser irradiation affects satellite cell proliferation and differentiation in vitro. Biochim Biophys Acta, Mol Cell Res 1448:372–380. https://doi.org/10.1016/S0167-4889(98)00147-5
17. Wu Y, Wang J, Gong D et al (2012) Effects of low-level laser irradiation on mesenchymal stem cell proliferation: a microarray analysis. Lasers Med Sci 27:509–519. https://doi.org/10.1007/s10103-011-0995-x
18. Zhang Y, Song S, Fong C-C et al (2003) cDNA microarray analysis of gene expression profiles in human fibroblast cells irradiated with red light. J Invest Dermatol 120:849–857. https://doi.org/10.1046/j.1523-1747.2003.12133.x
19. Trapnell C, Roberts A, Goff L et al (2012) Differential gene and transcript expression analysis of RNA-seq experiments with TopHat and cufflinks. Nat Protoc 7:562–578. https://doi.org/10.1038/nprot.2012.016
20. Shannon P, Markiel A, Ozier O et al (2003) Cytoscape: a software environment for integrated models of biomolecular interaction networks. Genome Res 13:2498–2504. https://doi.org/10.1101/gr.1239303
21. Bindea G, Mlecnik B, Hackl H et al (2009) ClueGO: a Cytoscape plug-in to decipher functionally grouped gene ontology and pathway annotation networks. Bioinformatics 25:1091–1093. https://doi.org/10.1093/bioinformatics/btp101
22. Aranda B, Blankenburg H, Kerrien S et al (2011) PSICQUIC and PSISCORE: accessing and scoring molecular interactions. Nat Methods 8:528–529. https://doi.org/10.1038/nmeth.1637
23. Bindea G, Galon J, Mlecnik B (2013) CluePedia Cytoscape plugin: pathway insights using integrated experimental and in silico data. Bioinformatics 29:661–663. https://doi.org/10.1093/bioinformatics/btt019
24. Chen EY, Tan CM, Kou Y et al (2013) Enrichr: interactive and collaborative HTML5 gene list enrichment analysis tool. BMC Bioinformatics 14:128. https://doi.org/10.1186/1471-2105-14-128
25. Kuleshov MV, Jones MR, Rouillard AD et al (2016) Enrichr: a comprehensive gene set enrichment analysis web server 2016 update. Nucleic Acids Res 44:W90–W97. https://doi.org/10.1093/nar/gkw377
26. Barrett T, Wilhite SE, Ledoux P et al (2013) NCBI GEO: archive for functional genomics data sets—update. Nucleic Acids Res 41:D991–D995. https://doi.org/10.1093/nar/gks1193
27. Edgar R, Domrachev M, Lash AE (2002) Gene Expression Omnibus: NCBI gene expression and hybridization array data repository. Nucleic Acids Res 30:207–210

28. Tomczak KK, Marinescu VD, Ramoni MF et al (2003) Expression profiling and identification of novel genes involved in myogenic differentiation. FASEB J 17. https://doi.org/10.1096/fj.03-0568fje
29. Yan Z, Choi S, Liu X et al (2003) Highly coordinated gene regulation in mouse skeletal muscle regeneration. J Biol Chem 278:8826–8836. https://doi.org/10.1074/jbc.M209879200
30. Silva LMG, Da Silva CAA, Da Silva A et al (2016) Photobiomodulation protects and promotes differentiation of C2C12 myoblast cells exposed to snake venom. PLoS One 11:1–16. https://doi.org/10.1371/journal.pone.0152890
31. Zanou N, Gailly P (2013) Skeletal muscle hypertrophy and regeneration: interplay between the myogenic regulatory factors (MRFs) and insulin-like growth factors (IGFs) pathways. Cell Mol Life Sci 70:4117–4130. https://doi.org/10.1007/s00018-013-1330-4
32. Albini S, Coutinho Toto P, Dall'Agnese A et al (2015) Brahma is required for cell cycle arrest and late muscle gene expression during skeletal myogenesis. EMBO Rep 16:1037–1050. https://doi.org/10.15252/embr.201540159
33. Guttridge DC, Albanese C, Reuther JY et al (1999) NF-kappaB controls cell growth and differentiation through transcriptional regulation of cyclin D1. Mol Cell Biol 19:5785–5799
34. Panda AC, Abdelmohsen K, Martindale JL et al (2016) Novel RNA-binding activity of MYF5 enhances *Ccnd1/Cyclin D1* mRNA translation during myogenesis. Nucleic Acids Res gkw023. https://doi.org/10.1093/nar/gkw023
35. Skapek SX, Rhee J, Spicer DB, Lassar AB (1995) Inhibition of myogenic differentiation in proliferating myoblasts by cyclin D1-dependent kinase. Science 267:1022–1024
36. Skapek SX, Rhee J, Kim PS et al (1996) Cyclin-mediated inhibition of muscle gene expression via a mechanism that is independent of pRB hyperphosphorylation. Mol Cell Biol 16:7043–7053
37. Zhang JM, Zhao X, Wei Q, Paterson BM (1999) Direct inhibition of G(1) cdk kinase activity by MyoD promotes myoblast cell cycle withdrawal and terminal differentiation. EMBO J 18:6983–6993. https://doi.org/10.1093/emboj/18.24.6983
38. Li Z, Gilbert JA, Zhang Y et al (2012) An HMGA2-IGF2BP2 axis regulates myoblast proliferation and myogenesis. Dev Cell 23:1176–1188. https://doi.org/10.1016/j.devcel.2012.10.019
39. Figeac N, Serralbo O, Marcelle C, Zammit PS (2014) ErbB3 binding protein-1 (Ebp1) controls proliferation and myogenic differentiation of muscle stem cells. Dev Biol 386:135–151. https://doi.org/10.1016/j.ydbio.2013.11.017
40. Tomczak KK, Marinescu VD, Ramoni MF et al (2004) Expression profiling and identification of novel genes involved in myogenic differentiation. FASEB J 18:403–405. https://doi.org/10.1096/fj.03-0568fje\r03-0568fje